A Burkholderia Type VI Effector Deamidates Rho GTPases to Activate the Pyrin Inflammasome

Aubert, D. F., Xu, H., Yang, J., Shi, X., Gao, W., Li, L., ... Shao, F. (2016). A Burkholderia Type VI Effector Deamidates Rho GTPases to Activate the Pyrin Inflammasome. Cell host & microbe, 19(5), 664-674. DOI: 10.1016/j.chom.2016.04.004

Published in:
Cell host & microbe

Document Version:
Peer reviewed version

A *Burkholderia* Type VI Effector Deamidates Rho GTPases to Activate the Pyrin Inflammasome

Daniel F. Aubert[1¶], Hao Xu[2¶], Jieling Yang[2, 4¶], Xuyan Shi[2], Wenqing Gao[2], Lin Li[2], Fabiana Bisaro[3], She Chen[2] Miguel A. Valvano[1, 3*], and Feng Shao[2, 5*]

[1] Department of Microbiology and Immunology, University of Western Ontario, London, N6A 5C1, Canada.

[2] National Institute of Biological Sciences, Beijing 102206, China.

[3] Centre for Infection and Immunity, Queen's University Belfast, Belfast, BT9 7AE, United Kingdom.

[4] National Laboratory of Biomacromolecules, Institute of Biophysics, Chinese Academy of Sciences, Beijing 100101, China.

[5] National Institute of Biological Sciences, Beijing, Collaborative Innovation Center for Cancer Medicine, Beijing 102206, China.

[¶] Equal contribution

* Correspondence: m.valvano@qub.ac.uk (M.A.V), shaofeng@nibs.ac.cn (F.S.).

Article Highlights

- *B. cenocepacia* employs a type VI effector TecA to disrupt actin cytoskeleton
- TecA inactivates Rho GTPases by deamidating Asn-41 in RhoA
- TecA defines a family of bacterial proteins with asparagine deamidase activity
- TecA deamidation of Rho GTPases triggers Pyrin inflammasome activation
- Detection of TecA by Pyrin protects mice from lethal *B. cenocepacia* infection

SUMMARY

Burkholderia cenocepacia employs a Type VI secretion system (T6SS) to survive in macrophages by disarming Rho-type GTPases, causing actin cytoskeletal defects. Here, we identified TecA (T6SS effector affecting cytoskeletal architecture), a non-VgrG T6SS effector responsible for disrupting actin cytoskeleton. TecA and other bacterial homologs bear a cysteine protease-like catalytic triad, which inactivates Rho GTPases by catalyzing deamidation of a specific asparagine in Rho. TecA deamidation of Rho activates the canonical inflammasome and pyroptotic cell death in infected macrophages and dendritic cells, which is mediated by the familial Mediterranean fever disease protein Pyrin. The physiological function of TecA is recapitulated in mouse lung infections, in which its deamidase activity is necessary and sufficient for *B. cenocepacia*-triggered lung inflammation. Detection of TecA by Pyrin is protective on mice from lethal *B. cenocepacia* infection. Therefore, *Burkholderia* TecA is a novel T6SS effector that modifies a eukaryotic target through a unique asparagine deamidase activity, which elicits host cell death and inflammation due to activation of the Pyrin inflammasome.

INTRODUCTION

The type VI-secretion system (T6SS) is a contractile nanomachine widely distributed in Gram-negative bacteria (Basler et al., 2012; Boyer et al., 2009; Clemens et al., 2015; Kudryashev et al., 2015; Zoued et al., 2014). The T6SS structurally resembles the bacteriophage tail injection device; the tail tube is made of the Hcp protein and a puncturing device containing proteins of the VgrG family and various VgrG-associated proteins caps the Hcp tube (Zoued et al., 2014). Upon cell contact, the T6SS delivers toxic effectors into neighboring target cells. Most of the known T6SS effectors act on bacterial competitors cells and include peptidoglycan-, membrane-, and nucleic acid-targeting enzymes (Durand et al., 2014; Russell et al., 2014).

Among T6SS effectors that act on eukaryotic cells, the "evolved" VgrG proteins (also required for assembly of the T6SS apparatus) are the most established. The *P. aeruginosa* VgrG2b contains a Zn^{2+}-dependent metalloprotease domain and interacts with tubulin components (Sana et al., 2015), while VgrG1 proteins from *Vibrio cholerae* and *Aeromonas hydrophila* contain an actin cross-linking domain (Durand et al., 2012) and an ADP-ribosylating domain (Suarez et al., 2010), respectively. Other evolved VgrGs from *V. parahaemolyticus* and *B. pseudomallei* have effects on autophagy and host cell fusion (Schwarz et al., 2014; Toesca et al., 2014; Yu et al., 2015) with unknown molecular mechanisms. In contrast, few non-VgrG T6SS effectors have been reported. The VasX protein from *V. cholerae* contains an N-terminal pleckstrin domain that interacts with phospholipids and can compromise the inner membrane of prokaryotic target cells (Miyata et al., 2011; Miyata et al., 2013); the PldA/B proteins from *P. aeruginosa* are phospholipases and their expression is associated with PI3K/Akt activation in infected

69 eukaryotic cells (Jiang et al., 2014); EvpP from *Edwarsiella tarda* is necessary for
70 virulence of the bacteria (Zheng and Leung, 2007). However, the physiological function
71 of these non-VgrG effectors is not well established and it remains to be conclusively
72 demonstrated that these proteins are bona fide T6SS effectors specifically modulating
73 eukaryotic host functions.

74 *Burkholderia cenocepacia* is an environmental Gram-negative opportunistic pathogen
75 that causes severe chronic lung infection in cystic fibrosis patients (Drevinek and
76 Mahenthiralingam, 2010). *B. cenocepacia* is pathogenic in plant and non-mammalian
77 animal infection models (Khodai-Kalaki et al., 2015; Uehlinger et al., 2009; Vergunst et
78 al., 2010), and survives intracellularly within amoebae and macrophages (Valvano et al.,
79 2012). Unlike other cystic fibrosis pathogens, *B. cenocepacia* does not form biofilms in
80 the lungs of infected patients and resides primarily within human mucosal macrophages
81 (Schwab et al., 2014). Intramacrophage *B. cenocepacia* delays phagosomal maturation,
82 alters the actin cytoskeleton, and triggers inflammation and cell death (Valvano et al.,
83 2012). *B. cenocepacia* infection and pathogenesis critically requires the function of a
84 T6SS. The *B. cenocepacia* T6SS inactivates Rho family GTPases, which reduces the
85 phagocytic capacity of macrophages (Flannagan et al., 2012; Rosales-Reyes et al., 2012),
86 blocks NADPH oxidase assembly onto the *B. cenocepacia*-containing vacuole (Keith et
87 al., 2009; Rosales-Reyes et al., 2012), and disrupts the macrophage's actin cytoskeleton
88 (Aubert et al., 2008; Flannagan et al., 2012; Rosales-Reyes et al., 2012). The T6SS also
89 leads to activation of the canonical caspase-1 inflammasome, interleukin (IL)-1/18
90 secretion and pyroptosis in macrophages (Gavrilin et al., 2012; Xu et al., 2014).
91 Pyroptosis is a programmed, necrotic cell death that causes exaggerated proinflammatory

responses and ultimately tissue damage. Inflammasome activation after *B. cenocepacia* infection in macrophages involves Pyrin (Xu et al., 2014), an intracellular innate immune sensor that detects pathogen-induced modifications of Rho GTPases (Xu et al., 2014; Yang et al., 2014). Interestingly, gain-of-function mutations in Pyrin are the cause for familial Mediterranean fever, an autoinflammatory disease in humans.

Despite the genetic requirement of the T6SS in *B. cenocepacia* for manipulating host function, no T6SS effectors involved in the cellular changes of infected macrophages have been identified. In fact, no effector-encoding genes appear to be present in the T6SS core cluster and neither the candidate VgrG nor VgrG-associated proteins are responsible for the actin cytoskeletal rearrangements (Aubert et al., 2015). Here, we performed genetic screen in *B. cenocepacia* and identified TecA (T6SS effector protein affecting cytoskeletal architecture), a non-VgrG T6SS effector with a unique deamidase activity. Specific deamidation by TecA of a critical asparagine residue in RhoA and Rac1 GTPases causes their inactivation and disruption of host actin cytoskeleton. TecA defines a novel family of bacterial cysteine protease-like enzymes that catalyze asparagine deamidation of Rho GTPases. TecA deamidation of RhoA drives activation of the Pyrin inflammasome in infected macrophages and dendritic cells. This innate immune response mediates lung inflammation during intranasal *B. cenocepacia* infection in mice, and can also protect the mice from lethal peritoneal *B. cenocepacia* infection. TecA is the first bacterial toxin secreted by an intracellular pathogen that targets the switch I region of Rho GTPases and inactivates their function by deamidation of an essential asparagine residue.

RESULTS

Identification of a non-VgrG T6SS effector in *B. cenocepacia* that drives host actin cytoskeleton rearrangements

B. cenocepacia infection disrupts the actin cytoskeleton in macrophages, forming "beads on a string"-like structures featuring long extensions with bleb-like structures located along the extensions and surrounding the cell periphery (Aubert et al., 2008; Flannagan et al., 2012; Rosales-Reyes et al., 2012). This phenotype reflects a collapse of the actin filaments in the lamellipodia and defective retraction during migration, and is dependent upon a functional T6SS (Aubert et al., 2008; Flannagan et al., 2012; Rosales-Reyes et al., 2012). The T6SS activity in *B. cenocepacia* can be stimulated by deleting AtsR (Adhesion and Type Six secretion system Regulator), a hybrid sensor kinase of a two-component system (Aubert et al., 2010; Aubert et al., 2008; Aubert et al., 2013; Khodai-Kalaki et al., 2013). This ensures uniform high expression of the T6SS genes and provides higher reproducibility of the results, especially in strain K56-2 that does not have a high macrophage infection index. Consistently, infection of macrophages with the Δ*atsR* mutant of *B. cenocepacia* K56-2 results in increased formation of "beads on a string"-like structures (Aubert et al., 2008; Flannagan et al., 2012; Rosales-Reyes et al., 2012). We recently developed a densitometry assay that quantifies the extent of this phenotype (Aubert et al., 2015). Using this assay, we performed random transposon mutagenesis screens in the Δ*atsR* background to search for bacterial mutants unable to induce disruption of the actin cytoskeleton in macrophages. 27 mutants were identified from the initial screen of 2,700 independent transposon mutants, and 6 of them (all having transposon insertions outside of the T6SS cluster) did not pass further

confirmation by targeted deletion of the gene disrupted by the transposon. Among the remaining 21 mutants incapable of inducing "beads on a string"-like structures, 20 had a transposon inserted into genes encoding critical core components of the T6SS apparatus (Figure 1A). The last insertion mutant was in BCAM1857 (GenBank: CAR55715.1), a gene located on chromosome 2 and outside of the T3SS locus (Figure 1A). Deletion of BCAM1857 in Δ*atsR* resulted in a strain unable to induce formation of the "beads on a string"-like structures in macrophages (Figure 1B-C). This phenotype could be restored to parental levels by introducing in the strain a plasmid expressing the BCAM1857 protein (Figure 1B-C). Therefore, BCAM1857 could be a putative non-VgrG T6SS effector responsible for cytoskeletal changes in macrophages and was renamed TecA (T6SS effector protein affecting cytoskeletal architecture).

Growth curves and gentamicin protection assays indicated that *B. cenocepacia* Δ*atsR*Δ*tecA* grows at a similar rate as the Δ*atsR* parent strain in LB medium as well as in immortalized murine macrophages (Figure S1A and S1B). Similar Hcp levels were detected in Δ*atsR* and Δ*atsR*Δ*tecA* culture supernatants, indicating that deletion of *tecA* does not affect the T6SS apparatus (Figure S1C). When overexpressed in Δ*atsR* and the isogenic T6SS-deficient Δ*atsR*Δ*hcp* mutant, low amounts of TecA were predominantly and reproducibly detected in culture supernatants of Δ*atsR* but not Δ*atsR*Δ*hcp* despite a similar TecA expression found in cell lysates of the two bacterial strains (Figure S1C). Chromosomally encoded TecA was not detectable initially in Δ*atsR* cell lysates by the routine immunoblotting assay (Figure S1C), but became detectable upon increasing sample loading and exposure time of the immunoblot (Figure S1D), suggesting a low

160 expression of TecA in *in vitro* cultured bacteria. Together, these data suggest the need of
161 a functional T6SS for TecA secretion, as expected for a bona fide T6SS effector protein.
162 Like *B. cenocepacia* K56-2, *B. multivorans* ATCC17616 also infects, survives and
163 replicates within macrophages (Schmerk and Valvano, 2013). *B. multivorans*
164 ATCC17616 possesses two T6SS clusters and an *atsR* ortholog (Bmul_5222, herein
165 named $atsR_{Bm}$), but lacks a *tecA* homolog. Culture supernatant of *B. multivorans*
166 ATCC17616 Δ$atsR_{Bm}$ showed a similar expression of Hcp as that of *B. cenocepacia* K56-
167 2 Δ*atsR*, suggesting that the T6SSs in *B. multivorans* ATCC17616 are functional (Figure
168 S1E). However, Δ$atsR_{Bm}$ could not induce the "beads on a string"-like phenotype in
169 infected macrophages (Figure 1D). Notably, heterologous expression of TecA in Δ$atsR_{Bm}$
170 enabled this bacterium to induce cytoskeletal rearrangements comparable to those found
171 in *B. cenocepacia* (Figure 1C-D). These data strongly indicate that T6SS-translocated
172 TecA is both necessary and sufficient to drive cytoskeletal defects in infected
173 macrophages.
174
175 ***B. cenocepacia* infection induces Asn-41 deamidation of RhoA due to a putative**
176 **T6SS effector activity**
177 *B. cenocepacia* K56-2 and J2135 are clonally related and often used indistinctly
178 (Mahenthiralingam et al., 2000). Unlike K56-2, J2315 lacks the ability to produce O
179 antigen lipopolysaccharide (Ortega et al., 2005) and consequently infects macrophages
180 more readily (Saldías et al., 2009). J2315 can induce similar "beads on a string"-like
181 structures in macrophages, which does not require deletion of *atsR*. We recently
182 discovered that intracellular J2315 infection resulted in the T6SS-dependent inactivation

of RhoA by inducing deamidation of asparagine-41 (Asn-41) (Xu et al., 2014), a residue located in the switch-I region of the GTPase. This observation was confirmed here by mass spectrometry analyses of FLAG-RhoA purified from murine dendritic DC2.4 cells infected with J2315 or its T6SS-defective Δ*hcp* mutant (Figure 2A). The *C. botulinum* ADP-ribosylation C3 toxin modifies Asn-41, generating a mobility shift of RhoA on SDS-polyacrylamide gels. This mobility shift provided a convenient assay, which confirmed the deamidation modification of RhoA induced J2315 infection (Figure 2A). Notably, we observed that RhoA from non-infected cells, upon incubation with cytosolic extracts of J2315 but not its Δ*Hcp* mutant-infected cells, also resisted C3 toxin modification (Figure 2B). The Rho-modifying activity could also be recapitulated from the pellets of J2315-infected macrophages (containing the bacteria and proteins expressed within the bacteria), but unlike the situation in the bacteria-free cytosol, the activity was not dependent on the T6SS (Figure 2C). Together, these data strongly indicate that *B. cenocepacia* expresses a T6SS effector that deamidates RhoA upon translocation from the bacteria into the host cytosol, also excluding the possibility that infection-induced RhoA deamidation is host-derived. Supporting this idea, we found that lysates of *in vitro* cultured *B. cenocepacia*, but not those of *E. coli* and *B. thailandensis*, showed a similar activity that renders RhoA resistant to further modification by the C3 toxin (Figure 2D). Consistently, RhoA recombinantly expressed and purified from *B. cenocepacia* showed a deamidation modification on Asn-41, contrasting to recombinant RhoA purified from the conventional *E. coli* host (Figure 2E).

The T6SS effector TecA mediates RhoA deamidation *in vivo* and *in vitro*

206 Also in the experiments described above, we found that RhoA purified from the Δ*tecA*
207 strain of *B. cenocepacia* was not deamidated and showed the same mass as that from *E.*
208 *coli* (Figure 2E), suggesting that TecA is the candidate T6SS effector that causes RhoA
209 deamidation. We further observed that deamidation of RhoA did not occur in DC2.4 cells
210 infected with the Δ*tecA* isogenic mutant of J2315, similarly as in infections with the Δ*hcp*
211 mutant (Figure 3A). Complementing TecA expression in Δ*tecA* by a *tecA*-encoding
212 plasmid restored the protection of RhoA from C3 toxin-catalyzed ADP-ribosylation
213 (Figure 3B). Further, introducing the TecA-expression plasmid in *B. thailandensis*, which
214 harbors a similar T6SS, resulted in the same modification of RhoA upon infection of
215 DC2.4 cells, which did not occur in cells infected with bacteria expressing the
216 enzymatically inactive $TecA_{C41A}$ (see below) (Figure 3C). These results demonstrate that
217 TecA is essential for the T6SS-mediated Asn-41 deamidation of RhoA. Exogenous
218 expression of TecA, but not $TecA_{C41A}$, in 293T cells recapitulated the same results as
219 those observed in infected DC2.4 cells (Figure 3D). Mass spectrometry of FLAG-RhoA
220 purified from 293T cells confirmed the conversion of Asn-41 into an aspartic acid
221 (Figure 3E). Same results were observed in *E. coli* co-expressing RhoA and the TecA or
222 $TecA_{C41A}$ proteins (Figure 3F). These data demonstrate that TecA is required and
223 sufficient for deamidation of the Asn-41 residue in RhoA.
224 Previous work showed that the *B. cenocepacia* T6SS is needed to deactivate the Rho-
225 family Rac1 and Cdc42 GTPases (Flannagan et al., 2012; Rosales-Reyes et al., 2012).
226 We therefore investigated Rac1 expressed in 293T cells together with TecA. Mass
227 spectrometry confirmed that the peptide containing Asn-39 in Rac1 (equivalent to Asn-41
228 in RhoA) was modified to aspartic acid by TecA (Figure 3G), indicating TecA causes the

same modification in other Rho-family members by targeting the conserved asparagine in the switch I region. Notably, when we transiently expressed the deamidated Rac1 (N39D) or RhoA (N41D) alone in 293T cells, the "beads on a string"-like structure was readily observed in cells expressing Rac1 N39D but not RhoA N41D (Figure 3H). These suggest that TecA-induced Rac1 deamidation and inactivation is responsible for the actin cytoskeleton disruption caused by *B. cenocepacia* infection.

The TecA effector defines a family of bacterial deamidases that modify Rho GTPases

TecA is a 159-amino acid protein of predicted unknown function. As expected for a T6SS substrate, TecA lacks a canonical N-terminal signal peptide. No putative conserved domains could be detected using PFAM and HHPred, and we also failed to identify any evident primary sequence similarity between TecA and known deamidases or other enzymes with hydrolytic activity. BLAST searches uncovered TecA orthologs in *B. cenocepacia* BC7, H111, AU1054, HI2424, H111, and MC0-3, (sharing over 91-99% amino acid identity with TecA of K56-2 and J2315), and in *B. contaminans*, *B. pyrrocinia*, *B. lata*, *B. cepacia* ATCC25416, *B. cenocepacia* PC184, and *B. ubonensis* (sharing 75-85% amino acid identity with TecA) (Figure 4A), suggesting that TecA is prevalent in a subset of *Burkholderia* species. Several additional homologs, sharing from 37 to 50% amino acid identity with TecA were also found in *Alcaligenes faecalis*, *Chryseobacterium indologenes*, the fish pathogen *Flavobacterium branchiophilum* FL-15, and the opportunistic pathogen and symbiont *Ochrobactrum anthropi* ATCC49188 (Figure 4A). Sequence alignments of these proteins revealed a conserved Cys-His-Asp

252 triad (Cys-41, His-105, and Asp-148 in TecA). The Cys-His-Asp/Asn/Glu/Gln triad
253 forms a catalytic pocket in many proteases and protease-like hydrolytic enzymes
254 including deamidases (Cui et al., 2010; Washington et al., 2013; Yao et al., 2012). The
255 cysteine, activated by the histidine and sometimes the nonessential third residue in the
256 triad, serves as the catalytic nucleophile. Interestingly, *in silico* structural modeling of
257 TecA using I-TASSER (Roy et al., 2010) revealed a similar structural fold with various
258 cysteine protease families including proteins containing the NlpC/P60, cysteine-histidine
259 hydrolase, and papain-like cysteine peptidase domains (PDB accessions 2EVR, 2FG0,
260 2HBW, 4F88, 3GQJ, and 3S0Q). The predicted TecA model revealed the putative
261 catalytic Cys-41 and His-105 residues situated in positions consistent with a catalytic
262 triad typical of cysteine proteases and protease-like hydrolases, further supporting the
263 hypothesis that TecA is a cysteine protease-like hydrolase (Figure 4B). Thus, despite the
264 lack of significant primary sequence similarity, TecA likely adopts a three-dimensional
265 fold characteristic of members of the cysteine protease family.

266 Mutagenesis was then carried out to test the deamidase activity of TecA and its
267 orthologs. Alanine substitution of Cys-41 and His-105 in TecA abrogated Asn-41
268 deamidation of RhoA and Rac1 in the 293T cells co-expression system (Figure 5A and
269 Figure 3D, 3E and G). The $TecA_{D148A}$ was partially active, but removal of the C-terminal
270 20 residues containing the Asp-148 resulted in a completely inactive enzyme (Figure 5A).
271 $TecA_{C41A}$ was also unable to deamidate Asn-41 in RhoA in the *E. coli* expression assay
272 (Figure 3F). Upon DC2.4 infection with *B. cenocepacia* or *B. thailandensis* strains
273 expressing the T6SS, TecAC41A failed to induce RhoA deamidation (Figure 3C and data
274 not shown). Co-expression of RhoA and TecA orthologues from *C. indologenes*

(WP_034735953), *F. branchiophilum* (WP_014085254), and *O. anthropi* (WP_011982319) in 293T cells gave the same results as with *B. cenocepacia* TecA, namely protection of RhoA from C3 toxin-mediated ADP-ribosylation (Figure 5B). Further, replacement of the putative catalytic Cys-40, His-104, or Asp-149 in WP_034735953 with alanine abrogated the protective effect on RhoA from C3 toxin-catalyzed modification (Figure 5C). Mass spectrometry confirmed that WP_034735953 deamidated RhoA and Rac1 in 293T cells at Asn-41 and Asn-39, respectively, and this modification did not occur with the C40A mutant protein (Figure 5D). Together, these results demonstrate that *B. cenocepacia* TecA epitomizes a family of bacterial proteins specifically catalyzing asparagine deamidation of Rho GTPases in mammalian cells.

TecA deamidation of RhoA mediates *B. cenocepacia*-induced Pyrin inflammasome activation

Our recent studies suggest that the Pyrin inflammasome senses Rho inactivation induced by bacterial Rho-modifying agents (Xu et al., 2014). Therefore, we examined whether TecA deamidation of host Rho GTPases could activate the Pyrin inflammasome. Confirming our previous observation (Xu et al., 2014), infection of primary mouse bone marrow macrophages (BMDMs) with *B. cenocepacia* J2315, but not the Δ*hcp* mutant, stimulated caspase-1 autoprocessing, pyroptotic cell death and IL-1β secretion (Figure 6A and 6B), hallmarks of canonical inflammasome activation. These proinflammatory responses were absent in BMDMs derived from *Mefv*$^{-/-}$ mice (*Mefv* is the gene encoding Pyrin). Importantly, the Δ*tecA* mutant strain behaved similarly as Δ*hcp*, failing to induce caspase-1 activation, pyroptosis and IL-1β secretion (Figure 6A and 6B). Restoring TecA

298 expression in Δ*tecA* restored *B. cenocepacia*-induced caspase-1 activation and pyroptosis
299 in primary BMDMs (Figure 6C and 6D). In contrast, TecA mutants in the three putative
300 catalytic residues (C41A, H105A and D148A) did not restore the infection-triggered
301 inflammasome responses (Figure 6C and 6D). Similar results were obtained with *B.*
302 *cenocepacia* infections in DC2.4 cells (Figure 6E). Furthermore, we generated the N41L
303 mutant of RhoA as well as the equivalent N39L mutants of Rac1 and Cdc42. When the
304 deamidation-resistant mutant Rho was overexpressed in DC2.4 cells, we found that RhoA
305 N41L could evidently inhibit *B. cenocepacia* infection-induced Pyrin inflammasome
306 activation (Figure 6F). In contrast, neither the N39L mutants of Rac1/Cdc42 nor wild-
307 type RhoA showed such dominant-negative effects (Figure 6F). These data are consistent
308 with our previous observation that modification of RhoA but not other GTPase substrates
309 induces Pyrin inflammasome activation (Xu et al., 2014), and strongly suggest that TecA-
310 mediated deamidation of RhoA is responsible for *B. cenocepacia*-stimulated Pyrin
311 inflammasome activation.
312
313 **TecA mediates *B. cenocepacia*-induced lung inflammation and its recognition by**
314 **Pyrin can protect mice from lethal infection**
315 Intranasal *B. cenocepacia* infection of wild-type mice triggered strong lung inflammation,
316 evidenced by massive infiltration of inflammatory cells, appearance of intra-alveolar
317 leukocytes, and destruction of the normal lung architecture due to activation of the Pyrin
318 inflammasome (Xu et al., 2014) (Figure 7A). In contrast, mice infected with *B.*
319 *cenocepacia* Δ*tecA* showed negligible lung inflammation. Expressing wild type but not
320 the deamidase-defective $TecA_{C41A}$ protein in the mutant bacteria restored the strong

inflammation in the infected lungs (Figure 7A). These observations were also evident from the clinical pathology scores that measure the lung damage (Figure 7B). Thus, the TecA deamidase activity induces Pyrin inflammasome-mediated inflammation due to its modification and inactivation of host Rho GTPases. To further demonstrate the functional significance of this innate immune recognition, peritoneal infection of mice with *B. cenocepacia* was performed. At the infection dose of 2×10^8 bacteria, nearly all the mice could resist wild-type *B. cenocepacia* infection, but the large majority of infected mice succumbed to the Δ*tecA* mutant bacteria (Figure 7C). The lethality is presumably caused by loss of the inflammation and consequently attenuated control of bacterial replication in the mice. Consistently, a higher number of *B. cenocepacia* Δ*tecA* than that of wild-type bacteria was recovered from the spleen of infected mice (Figure 7D). The bacterial loads in the liver showed a similar trend despite that the difference was not statistically significant. When the infection was performed with the *Mefv*$^{-/-}$ mice, wild-type *B. cenocepacia* infection also became lethal and showed a comparable lethality as the Δ*tecA* mutant bacteria (Figure 7C). These results highlight the protective role of Pyrin inflammasome that functions through detecting the Rho deamidase activity of TecA in *B. cenocepacia*.

DISCUSSION

We show that TecA is a single, non-VgrG T6SS effector protein that elicits actin cytoskeletal defects, inflammation, and macrophage pyroptosis by inactivating Rho GTPases through deamidation of an asparagine residue within the GTPase switch I region. Rho GTPases are central molecular switches of eukaryotic cells that cycle

between the inactive GDP-bound and active GTP-bound states and regulate key signaling pathways concerning cytoskeletal dynamics, trafficking, immune responses, and cell proliferation (Aktories, 2011). Not unexpectedly, many microbes produce proteins that target Rho GTPase signaling either by direct covalent modification of the GTPases or by manipulating their upstream and downstream regulators and effectors (Aktories, 2011). Pathogen effectors can block Rho GTPases activation, causing inhibition of cell migration and phagocytosis and disruption of the actin cytoskeleton, while in other cases can activate the GTPases to mediate bacterial entry into the cytosol. Alteration of the actin cytoskeletal dynamics is a typical cellular response to both inactivated and activated Rho GTPases, and recent evidence suggests that pathogen-induced "unnatural" actin dynamics is sensed by host innate immunity. For example, activation of Rac1/Cdc42 by the *Salmonella enterica* Type III effector SopE stimulates host NOD1 signaling leading to the induction of NF-κB-dependent inflammatory responses (Keestra et al., 2013), while RhoA inactivation causes Pyrin inflammasome activation (Xu et al., 2014).

TecA defines a new family of bacterial deamidases that are deployed by the T6SS upon bacterial intracellular infection. Enzymatic deamidation is a common pathogenic strategy utilized by a broad range of bacterial pathogens that infect plants and animals (Washington et al., 2013). Deamidation causes the replacement of an amide group with a carboxylate group, converting glutamine and asparagine into glutamic acid and aspartic acid, respectively. Several families of bacterial deamidases are known, which target various eukaryotic proteins that play key roles in cellular physiology. *E. coli* (CNF1, CFN2, CNF3) and *Yersinia pseudotuberculosis* (CNFY) cytotoxic necrotizing factors (Flatau et al., 1997; Lockman et al., 2002; Schmidt et al., 1997) and the *Vibrio*

367 *parahaemolyticus* type III effector VopC (Zhang et al., 2012) target a glutamine residue
368 in the switch II domain of Rho GTPases, which leads to constitutive activation resulting
369 in cytoskeletal rearrangements. BLF1 is a lethal toxin from *B. pseudomallei* that inhibits
370 host protein synthesis via deamidation of the translation factor eIF4A (Cruz-Migoni et al.,
371 2011). *Pasteurella multocida* toxin PMT activates heterotrimeric G proteins affecting
372 several downstream signaling pathways (Orth et al., 2009). Further, cell cycle-inhibiting
373 factors from multiple bacterial species inhibit ubiquitination pathways by deamidating
374 Glu-40 of ubiquitin and the ubiquitin-like protein NEDD8 (Cui et al., 2010), while
375 *Shigella flexneri* has evolved a type III effector protein that dampens TRAF6-mediated
376 immune responses by deamidating UBC13 (Sanada et al., 2012). It is worth noting that
377 TecA is the first known bacterial deamidase with specificity for asparagine and an
378 inhibitory effect on Rho GTPases.

379 TecA and its orthologs do not share primary amino acid sequence homology with
380 other known bacterial deamidases, and represent a novel class of deamidases. The TecA
381 family has a putative catalytic triad consisting of invariant cysteine, histidine and aspartic
382 acid residues, characteristic of the papain-like superfamily of hydrolytic enzymes
383 (Washington et al., 2013). Like other bacterial deamidases acting on Rho GTPases such
384 as CNF1 and CNFY, both RhoA and Rac1 can be TecA substrates. Previous data indicate
385 that Cdc42 is inactivated by the *B. cenocepacia* T6SS in murine macrophages (Flannagan
386 et al., 2012; Rosales-Reyes et al., 2012), suggesting that this GTPase might also be a
387 TecA substrate. As with CNFI (Flatau et al., 2000), TecA likely recognizes a relatively
388 short, common structural element in the switch-I region that would explain its ability to

work with multiple substrates, but additional experimentation is required to investigate this hypothesis.

Deamidation is enzymatically irreversible, making deamidases potent virulence factors (Washington et al., 2013). This is underscored by the robust effect of TecA on the innate immune responses and inflammation, as we have observed in infected macrophages and mice. The pro-inflammatory potential of *B. cenocepacia* has long been recognized, especially in the context of cystic fibrosis (Abdulrahman et al., 2011; Downey et al., 2007; Kopp et al., 2012). Our results convincingly demonstrate that lung inflammation upon *B. cenocepacia* infection depends on an enzymatically active TecA and highlight the importance of the Pyrin inflammasome in innate immune detection of *B. cenocepacia* (Xu et al., 2014). Indeed, Pyrin responds to pathogen modification and inactivation of Rho GTPases, which echoes the "guard hypothesis" in plant immunity (Xu et al., 2014; Yang et al., 2014). The effect of TecA-mediated Rho deamidation on the actin cytoskeleton of *B. cenocepacia*-infected cells and the fact that Pyrin and the Pyrin-ASC complexes localize to actin filaments (Mansfield et al., 2001; Waite et al., 2009), strongly suggest that Pyrin could be a sensor for actin homeostasis. In this context, the identification of TecA also provides a tool for future dissection of the pathway leading to Pyrin inflammasome activation.

EXPERIMENTAL PROCEDURES

Bacterial strains and plasmids

Strains and plasmids used in this study are listed in Table S1. Details on bacterial growth conditions, DNA transformation and triparental mating, and the cloning of TecA, RhoA and Rac1 coding sequences are also in the Supplementary Experimental Procedures.

Deletion and transposon mutagenesis

Unmarked and non-polar deletions in *B. cenocepacia* K56-2 and J2315 strains, and in *B. multivorans* ATCC17616 were performed as described previously (Flannagan et al., 2008; Hamad et al., 2010). Random transposon mutagenesis in *B. cenocepacia* K56-2 Δ*atsR* was performed using the pTn*Mod*-RTp' plasposon (Dennis and Zylstra, 1998). For further details, see the Supplementary Experimental Procedures.

Cell culture and transfection

293T cells and mouse BMDMs were cultured in DMEM (HyClone), while mouse DC2.4 dendritic cells were cultured in RPMI-1640. Details on culturing conditions and transfection are in the Supplementary Experimental Procedures.

Macrophage infections

To quantify the T6SS-dependent "beads on a string" phenotype (Aubert et al., 2015), infections were performed in the C57BL/6 murine bone marrow-derived macrophage cell line ANA-1 (Cox et al., 1989). Infection of DC2.4 dendritic cells and iBMDM cells was used to determine RhoA modification and inflammasome activation. Additional details are presented in Supplementary Experimental Procedures.

Hcp and TecA polyclonal antibodies and immunoblot analysis of TecA secretion

Hcp was PCR amplified and cloned into pET30a by use of NdeI and HindIII restriction sites, and introduced into *E. coli* strain BL21 (DE3) by transformation, generating pDA44. Hcp fused to 6xHis was purified and used to raise rabbit polyclonal antibodies. The peptide TRFNFETGDQWDGR from TecA was synthesized by ProSci Inc. (Poway, CA) and employed for rabbit immunization. See further details in Supplementary Experimental Procedures.

Inflammasome activation assays

Culture supernatants of primary BMDMs or EGFP-Pyrin-expressing DC2.4 cells that had been treated with indicated inflammasome stimuli were subjected to 15% trichloroacetic acid precipitation. Precipitates were analysed by anti-caspase-1 immunoblotting, and the total cell lysates were analyzed by anti-β-tubulin blotting as the loading control. IL-1β secretion was measured using the IL-1β ELISA kit (Neobioscience Technology Company). To determine pyroptotic cell death, the lactate dehydrogenase (LDH) assay was employed using the CytoTox 96 Non-Radioactive Cytotoxicity Assay kit (Promega).

Purification of recombinant proteins and *in vitro* deamidation reaction

His-tagged proteins were purified by affinity chromatography using Ni-NTA beads (Qiagen). For *in vitro* deamidation reaction, parental or mutant TecA recombinant proteins were incubated for 30 min at 37°C with RhoA (1:10 molar ratio) in a buffer made of 50 mM Tris-HCl (pH 7.5) and 150 mM NaCl. The resulting modified Rho proteins were subjected to mass spectrometry analyses directly or reaction with the C3

toxin. Approximately 0.1 μg of C3 toxin-reacted RhoA was separated on 15% SDS-PAGE gels followed by anti-RhoA immunoblotting. See further details in Supplementary Experimental Procedures.

Gel shift assay of RhoA ADP-ribosylation by the C3 toxin

DC2.4 or 293T cells were lysed by sonication in a buffer containing 20 mM Tris-HCl (pH 7.5), 150 mM NaCl, 20 mM β-OG and a protease inhibitor cocktail. The lysates were cleared by centrifugation at 16,000 g for 10 min. 15 μl of the supernatants were incubated with1 μg of recombinant C3 toxin with NAD and thymidine for 15 min at 30 °C and the reaction was stopped by adding SDS sample buffer. Cells lysates were separated by SDS-PAGE in 15% SDS-polyacrylamide gels and analyzed by immunoblotting.

Mice infections

Cultures of *B. cenocepacia* J2315, Δ*tecA* or Δ*tecA* complemented with pTecA were used to infect C57BL/6 wild-type or *Mefv*$^{-/-}$ mice intranasally to examine lung inflammation or intraperitoneally to investigate the lethal effect and bacteria loads. Lungs were removed for histopathology and sections stained with haematoxylin and eosin, and the damage of infected lungs was quantified by blindly scoring of the pathology. See further details in Supplementary Experimental Procedures. Animal experiments were conducted following the Ministry of Health national guidelines for housing and care of laboratory animals and performed in accordance with institutional regulations after review and approval by the Institutional Animal Care and Use Committee at National Institute of Biological Sciences.

SUPPLEMENTAL INFORMATION

Supplemental Information includes Supplementary Experimental Procedures, Supplementary Figure 1 and Supplementary Table 1.

AUTHOR CONTRIBUTIONS

M.A.V. and F.S. conceived the study; D.F.A., H. X. and J.Y. performed the majority of experiments; H.X. was assisted by W.G. X.S. performed mouse lethality and bacterial load assays. L.L. and S.C. performed the mass spectrometry analyses. F.B. provided technical assistance during the revision process. D.F.A., H. X., J.Y., M.A.V and F.S. analyzed the data and wrote the manuscript. All authors discussed the results and commented on the manuscript.

ACKNOWLEDGEMENTS

We thank members of the Shao laboratory for helpful discussions and technical assistance. This work was supported by grants from Cystic Fibrosis Canada and the UK Cystic Fibrosis Trust (to M.A.V) and grants from the Strategic Priority Research Program of the Chinese Academy of Sciences (XDB08020202), the China National Science Foundation Program for Distinguished Young Scholars (31225002), the Program for International Collaborations (31461143006), and the National Basic Research Program of China 973 Program (2012CB518700 and 2014CB849602) to F.S. M.A.V. was a Canada Research Chair in Infectious Diseases and Microbial Pathogenesis. F.S. was also

501 supported in part by an International Early Career Scientist grant from the Howard
502 Hughes Medical Institute (55007431) and the Beijing Scholar Program.
503

REFERENCES

Abdulrahman, B.A., Khweek, A.A., Akhter, A., Caution, K., Kotrange, S., Abdelaziz, D.H., Newland, C., Rosales-Reyes, R., Kopp, B., McCoy, K., *et al.* (2011). Autophagy stimulation by rapamycin suppresses lung inflammation and infection by *Burkholderia cenocepacia* in a model of cystic fibrosis. Autophagy *7*, 1359-1370.

Aktories, K. (2011). Bacterial protein toxins that modify host regulatory GTPases. Nat Rev Microbiol *9*, 487-498.

Aubert, D., MacDonald, D.K., and Valvano, M.A. (2010). BcsKC is an essential protein for the type VI secretion system activity in *Burkholderia cenocepacia* that forms an outer membrane complex with BcsLB. The Journal of biological chemistry *285*, 35988-35998.

Aubert, D.F., Flannagan, R.S., and Valvano, M.A. (2008). A novel sensor kinase-response regulator hybrid controls biofilm formation and virulence in *Burkholderia cenocepacia*. Infect Immun *76*, 1979-1991.

Aubert, D.F., Hu, S., and Valvano, M.A. (2015). Quantification of Type VI secretion system activity in macrophages infected with Burkholderia cenocepacia. Microbiology *161*, 2161-2173.

Aubert, D.F., O'Grady, E.P., Hamad, M.A., Sokol, P.A., and Valvano, M.A. (2013). The *Burkholderia cenocepacia* sensor kinase hybrid AtsR is a global regulator modulating quorum-sensing signalling. Environ Microbiol *15*, 372-385.

Basler, M., Pilhofer, M., Henderson, G.P., Jensen, G.J., and Mekalanos, J.J. (2012). Type VI secretion requires a dynamic contractile phage tail-like structure. Nature *483*, 182-186.

Boyer, F., Fichant, G., Berthod, J., Vandenbrouck, Y., and Attree, I. (2009). Dissecting the bacterial type VI secretion system by a genome wide in silico analysis: what can be learned from available microbial genomic resources? BMC Genomics *10*, 104.

Clemens, D.L., Ge, P., Lee, B.Y., Horwitz, M.A., and Zhou, Z.H. (2015). Atomic structure of T6SS reveals interlaced array essential to function. Cell *160*, 940-951.

Cox, G.W., Mathieson, B.J., Gandino, L., Blasi, E., Radzioch, D., and Varesio, L. (1989). Heterogeneity of hematopoietic cells immortalized by v-myc/v-raf recombinant retrovirus infection of bone marrow or fetal liver. Journal of the National Cancer Institute *81*, 1492-1496.

Cruz-Migoni, A., Hautbergue, G.M., Artymiuk, P.J., Baker, P.J., Bokori-Brown, M., Chang, C.T., Dickman, M.J., Essex-Lopresti, A., Harding, S.V., Mahadi, N.M., *et al.* (2011). A *Burkholderia pseudomallei* toxin inhibits helicase activity of translation factor eIF4A. Science *334*, 821-824.

539 Cui, J., Yao, Q., Li, S., Ding, X., Lu, Q., Mao, H., Liu, L., Zheng, N., Chen, S., and Shao,
540 F. (2010). Glutamine deamidation and dysfunction of ubiquitin/NEDD8 induced by a
541 bacterial effector family. Science *329*, 1215-1218.

542 Dennis, J.J., and Zylstra, G.J. (1998). Plasposons: modular self-cloning minitransposons
543 derivatives for rapid genetic analysis of gram-negative bacterial genomes. Appl Environ
544 Microbiol *64*, 2710-2715.

545 Downey, D.G., Martin, S.L., Dempster, M., Moore, J.E., Keogan, M.T., Starcher, B.,
546 Edgar, J., Bilton, D., and Elborn, J.S. (2007). The relationship of clinical and
547 inflammatory markers to outcome in stable patients with cystic fibrosis. Pediatric
548 pulmonology *42*, 216-220.

549 Drevinek, P., and Mahenthiralingam, E. (2010). *Burkholderia cenocepacia* in cystic
550 fibrosis: epidemiology and molecular mechanisms of virulence. Clin Microbiol Infect *16*,
551 821-830.

552 Durand, E., Cambillau, C., Cascales, E., and Journet, L. (2014). VgrG, Tae, Tle, and
553 beyond: the versatile arsenal of Type VI secretion effectors. Trends Microbiol *22*, 498-
554 507.

555 Durand, E., Derrez, E., Audoly, G., Spinelli, S., Ortiz-Lombardia, M., Raoult, D.,
556 Cascales, E., and Cambillau, C. (2012). Crystal structure of the VgrG1 actin cross-linking
557 domain of the *Vibrio cholerae* type VI secretion system. The Journal of biological
558 chemistry *287*, 38190-38199.

559 Flannagan, R.S., Jaumouillé, V., Huynh, K.K., Plumb, J.D., Downey, G.P., Valvano,
560 M.A., and Grinstein, S. (2012). *Burkholderia cenocepacia* disrupts host cell actin
561 cytoskeleton by inactivating Rac and Cdc42. Cell Microbiol *14*, 239-254.

562 Flannagan, R.S., Linn, T., and Valvano, M.A. (2008). A system for the construction of
563 targeted unmarked gene deletions in the genus *Burkholderia*. Environ Microbiol *10*,
564 1652-1660.

565 Flatau, G., Landraud, L., Boquet, P., Bruzzone, M., and Munro, P. (2000). Deamidation
566 of RhoA glutamine 63 by the *Escherichia coli* CNF1 toxin requires a short sequence of
567 the GTPase switch 2 domain. Biochem Biophys Res Commun *267*, 588-592.

568 Flatau, G., Lemichez, E., Gauthier, M., Chardin, P., Paris, S., Fiorentini, C., and Boquet,
569 P. (1997). Toxin-induced activation of the G protein p21 Rho by deamidation of
570 glutamine. Nature *387*, 729-733.

571 Gavrilin, M.A., Abdelaziz, D.H., Mostafa, M., Abdulrahman, B.A., Grandhi, J., Akhter,
572 A., Abu Khweek, A., Aubert, D.F., Valvano, M.A., Wewers, M.D.*, et al.* (2012).
573 Activation of the pyrin inflammasome by intracellular *Burkholderia cenocepacia*. J
574 Immunol *188*, 3469-3477.

Hamad, M.A., Skeldon, A.M., and Valvano, M.A. (2010). Construction of aminoglycoside-sensitive *Burkholderia cenocepacia* strains for use in studies of intracellular bacteria with the gentamicin protection assay. Appl Environ Microbiol *76*, 3170-3176.

Jiang, F., Waterfield, N.R., Yang, J., Yang, G., and Jin, Q. (2014). A *Pseudomonas aeruginosa* Type VI Secretion Phospholipase D Effector Targets Both Prokaryotic and Eukaryotic Cells. Cell Host Microbe *15*, 600-610.

Keestra, A.M., Winter, M.G., Auburger, J.J., Frassle, S.P., Xavier, M.N., Winter, S.E., Kim, A., Poon, V., Ravesloot, M.M., Waldenmaier, J.F.*, et al.* (2013). Manipulation of small Rho GTPases is a pathogen-induced process detected by NOD1. Nature *496*, 233-237.

Keith, K.E., Hynes, D.W., Sholdice, J.E., and Valvano, M.A. (2009). Delayed association of the NADPH oxidase complex with macrophage vacuoles containing the opportunistic pathogen *Burkholderia cenocepacia*. Microbiology *155*, 1004-1015.

Khodai-Kalaki, M., Andrade, A., Fathy Mohamed, Y., and Valvano, M.A. (2015). Burkholderia cenocepacia Lipopolysaccharide Modification and Flagellin Glycosylation Affect Virulence but Not Innate Immune Recognition in Plants. MBio *6*, e00679.

Khodai-Kalaki, M., Aubert, D.F., and Valvano, M.A. (2013). Characterization of the AtsR hybrid sensor kinase phosphorelay pathway and identification of its response regulator in *Burkholderia cenocepacia*. The Journal of biological chemistry *288*, 30473-30484.

Kopp, B.T., Abdulrahman, B.A., Khweek, A.A., Kumar, S.B., Akhter, A., Montione, R., Tazi, M.F., Caution, K., McCoy, K., and Amer, A.O. (2012). Exaggerated inflammatory responses mediated by *Burkholderia cenocepacia* in human macrophages derived from Cystic fibrosis patients. Biochem Biophys Res Commun *424*, 221-227.

Kudryashev, M., Wang, R.Y., Brackmann, M., Scherer, S., Maier, T., Baker, D., DiMaio, F., Stahlberg, H., Egelman, E.H., and Basler, M. (2015). Structure of the type VI secretion system contractile sheath. Cell *160*, 952-962.

Lockman, H.A., Gillespie, R.A., Baker, B.D., and Shakhnovich, E. (2002). *Yersinia pseudotuberculosis* produces a cytotoxic necrotizing factor. Infect Immun *70*, 2708-2714.

Mahenthiralingam, E., Coenye, T., Chung, J.W., Speert, D.P., Govan, J.R., Taylor, P., and Vandamme, P. (2000). Diagnostically and experimentally useful panel of strains from the *Burkholderia cepacia* complex. J Clin Microbiol *38*, 910-913.

Mansfield, E., Chae, J.J., Komarow, H.D., Brotz, T.M., Frucht, D.M., Aksentijevich, I., and Kastner, D.L. (2001). The familial Mediterranean fever protein, pyrin, associates with microtubules and colocalizes with actin filaments. Blood *98*, 851-859.

611 Miyata, S.T., Kitaoka, M., Brooks, T.M., McAuley, S.B., and Pukatzki, S. (2011). Vibrio
612 cholerae requires the type VI secretion system virulence factor VasX to kill
613 Dictyostelium discoideum. Infect Immun *79*, 2941-2949.

614 Miyata, S.T., Unterweger, D., Rudko, S.P., and Pukatzki, S. (2013). Dual expression
615 profile of type VI secretion system immunity genes protects pandemic Vibrio cholerae.
616 PLoS Pathog *9*, e1003752.

617 Ortega, X., Hunt, T.A., Loutet, S., Vinion-Dubiel, A.D., Datta, A., Choudhury, B.,
618 Goldberg, J.B., Carlson, R., and Valvano, M.A. (2005). Reconstitution of O-specific
619 lipopolysaccharide expression in the *Burkholderia cenocepacia* strain J2315 that is
620 associated with transmissible infections in patients with cystic fibrosis. J Bacteriol *187*,
621 1324-1333.

622 Orth, J.H., Preuss, I., Fester, I., Schlosser, A., Wilson, B.A., and Aktories, K. (2009).
623 *Pasteurella multocida* toxin activation of heterotrimeric G proteins by deamidation. Proc
624 Natl Acad Sci U S A *106*, 7179-7184.

625 Rosales-Reyes, R., Skeldon, A.M., Aubert, D.F., and Valvano, M.A. (2012). The Type
626 VI secretion system of *Burkholderia cenocepacia* targets multiple Rho family GTPases
627 disrupting the actin cytoskeleton and the assembly of NADPH oxidase complex in
628 macrophages. Cell Microbiol *14*, 255-273.

629 Roy, A., Kucukural, A., and Zhang, Y. (2010). I-TASSER: a unified platform for
630 automated protein structure and function prediction. Nat Protoc *5*, 725-738.

631 Russell, A.B., Peterson, S.B., and Mougous, J.D. (2014). Type VI secretion system
632 effectors: poisons with a purpose. Nat Rev Microbiol *12*, 137-148.

633 Saldías, M.S., Ortega, X., and Valvano, M.A. (2009). *Burkholderia cenocepacia* O
634 antigen lipopolysaccharide prevents phagocytosis by macrophages and adhesion to
635 epithelial cells. Journal of medical microbiology *58*, 1542-1548.

636 Sana, T.G., Baumann, C., Merdes, A., Soscia, C., Rattei, T., Hachani, A., Jones, C.,
637 Bennett, K.L., Filloux, A., Superti-Furga, G.*, et al.* (2015). Internalization of
638 *Pseudomonas aeruginosa* Strain PAO1 into Epithelial Cells Is Promoted by Interaction of
639 a T6SS Effector with the Microtubule Network. MBio *6*, e00712.

640 Sanada, T., Kim, M., Mimuro, H., Suzuki, M., Ogawa, M., Oyama, A., Ashida, H.,
641 Kobayashi, T., Koyama, T., Nagai, S.*, et al.* (2012). The *Shigella flexneri* effector OspI
642 deamidates UBC13 to dampen the inflammatory response. Nature *483*, 623-626.

643 Schmerk, C.L., and Valvano, M.A. (2013). *Burkholderia multivorans* survival and
644 trafficking within macrophages. J Med Microbiol *62*, 173-184.

645 Schmidt, G., Sehr, P., Wilm, M., Selzer, J., Mann, M., and Aktories, K. (1997). Gln 63 of
646 Rho is deamidated by *Escherichia coli* cytotoxic necrotizing factor-1. Nature *387*, 725-
647 729.

Schwab, U., Abdullah, L.H., Perlmutt, O.S., Albert, D., Davis, C.W., Arnold, R.R., Yankaskas, J.R., Gilligan, P., Neubauer, H., Randell, S.H.*, et al.* (2014). Localization of *Burkholderia cepacia* complex bacteria in cystic fibrosis lungs and interactions with *Pseudomonas aeruginosa* in hypoxic mucus. Infect Immun *82*, 4729-4745.

Schwarz, S., Singh, P., Robertson, J.D., LeRoux, M., Skerrett, S.J., Goodlett, D.R., West, T.E., and Mougous, J.D. (2014). VgrG-5 is a *Burkholderia* type VI secretion system-exported protein required for multinucleated giant cell formation and virulence. Infect Immun *82*, 1445-1452.

Suarez, G., Sierra, J.C., Erova, T.E., Sha, J., Horneman, A.J., and Chopra, A.K. (2010). A type VI secretion system effector protein, VgrG1, from *Aeromonas hydrophila* that induces host cell toxicity by ADP ribosylation of actin. J Bacteriol *192*, 155-168.

Toesca, I.J., French, C.T., and Miller, J.F. (2014). The Type VI secretion system spike protein VgrG5 mediates membrane fusion during intercellular spread by pseudomallei group *Burkholderia* species. Infect Immun *82*, 1436-1444.

Uehlinger, S., Schwager, S., Bernier, S.P., Riedel, K., Nguyen, D.T., Sokol, P.A., and Eberl, L. (2009). Identification of specific and universal virulence factors in Burkholderia cenocepacia strains by using multiple infection hosts. Infect Immun *77*, 4102-4110.

Valvano, M.A., Rosales-Reyes, R., Schmerk, C.L., and Ostapska, H. (2012). Molecular mechanisms of virulence of *Burkholderia cepacia* complex bacteria. In *Burkholderia*: From Genomes to Function, T. Coeyne, and E. Mahenthiralingam, eds. (Norfolk, UK., Caister Academic Press), pp. 149-160.

Vergunst, A.C., Meijer, A.H., Renshaw, S.A., and O'Callaghan, D. (2010). Burkholderia cenocepacia creates an intramacrophage replication niche in zebrafish embryos, followed by bacterial dissemination and establishment of systemic infection. Infect Immun *78*, 1495-1508.

Waite, A.L., Schaner, P., Hu, C., Richards, N., Balci-Peynircioglu, B., Hong, A., Fox, M., and Gumucio, D.L. (2009). Pyrin and ASC co-localize to cellular sites that are rich in polymerizing actin. Experimental biology and medicine *234*, 40-52.

Washington, E.J., Banfield, M.J., and Dangl, J.L. (2013). What a difference a Dalton makes: bacterial virulence factors modulate eukaryotic host cell signaling systems via deamidation. Microbiology and molecular biology reviews : MMBR *77*, 527-539.

Xu, H., Yang, J., Gao, W., Li, L., Li, P., Zhang, L., Gong, Y.N., Peng, X., Xi, J.J., Chen, S.*, et al.* (2014). Innate immune sensing of bacterial modifications of Rho GTPases by the Pyrin inflammasome. Nature *513*, 237-241.

Yang, J., Xu, H., and Shao, F. (2014). The immunological function of familial Mediterranean fever disease protein Pyrin. Science China Life sciences *57*, 1156-1161.

Yao, Q., Cui, J., Wang, J., Li, T., Wan, X., Luo, T., Gong, Y.N., Xu, Y., Huang, N., and Shao, F. (2012). Structural mechanism of ubiquitin and NEDD8 deamidation catalyzed by bacterial effectors that induce macrophage-specific apoptosis. Proc Natl Acad Sci U S A *109*, 20395-20400.

Yu, Y., Fang, L., Zhang, Y., Sheng, H., and Fang, W. (2015). VgrG2 of type VI secretion system 2 of *Vibrio parahaemolyticus* induces autophagy in macrophages. Frontiers in microbiology *6*, 168.

Zhang, L., Krachler, A.M., Broberg, C.A., Li, Y., Mirzaei, H., Gilpin, C.J., and Orth, K. (2012). Type III effector VopC mediates invasion for *Vibrio* species. Cell reports *1*, 453-460.

Zheng, J., and Leung, K.Y. (2007). Dissection of a type VI secretion system in *Edwardsiella tarda*. Mol Microbiol *66*, 1192-1206.

Zoued, A., Brunet, Y.R., Durand, E., Aschtgen, M.S., Logger, L., Douzi, B., Journet, L., Cambillau, C., and Cascales, E. (2014). Architecture and assembly of the Type VI secretion system. Biochim Biophys Acta *1843*, 1664-1673.

FIGURE LEGENDS

Figure 1. Identification of *tecA* Encoding A Novel Non-VgrG T6SS Effector Functioning in Eukaryotic Host Cells.

(A) Genetic map of the *B. cenocepacia* K56-2 T6SS gene cluster located on chromosome 1 (Chr. 1) and the *tecA* (BCAM1857) region on chromosome 2 (Chr. 2). Arrows indicate direction of transcription of each gene. Genes outside the T6SS cluster are indicated in black. *hcp* and *tecA* are highlighted in red. White circles indicate the position of the transposon insertion.

(B) Phase-contrast microscopy of ANA-1 macrophages at 4 h post-infection (MOI of 50) with *B. cenocepacia* K56-2 Δ*atsR* and Δ*atsR*Δ*tecA* carrying the vector control pDA12 or complementing plasmid pTecA. The arrows indicate "beads on a string"-like structures.

(C) Quantification of the development of "beads on a string"-like structures in *B. cenocepacia*-infected ANA-1 macrophages. Results were expressed in arbitrary units relative to Δ*atsR* set as 1. Values are mean ± standard deviation from at least 21 fields of view, and representative of three independent experiments. Cells infected with *B. cenocepacia* K56-2 Δ*atsR*Δ*hcp* were used as negative control.

(D) Phase-contrast microscopy of ANA-1 macrophages infected with *B. multivorans* Δ$atsR_{Bm}$ using the same conditions as in (B). The arrows mark the "beads on a string"-like structures.

See also Figure S1.

Figure 2. A T6SS-dependent Activity in *B. cenocepacia* That Leads to Rho Deamidation.

(A) T6SS-dependent Asn-41 deamidation of RhoA during *B. cenocepacia* infection. FLAG-RhoA was stably expressed and purified from DC2.4 cells infected with *B. cenocepacia* J2315 or its Δ*hcp* mutant, and analysed by mass spectrometry. The upper panel shows the extracted ion chromatograms of the Asn-41-containing peptide. The lower panel shows the behavior of endogenous RhoA in response to further modification by the C3 toxin.

(B) RhoA modification by cytosolic extracts of *B. cenocepacia*-infected cells. RhoA purified from non-infected DC2.4 cells was incubated with cytosolic extracts of DC2.4 cells infected with J2315 or Δ*hcp*, and then subjected to further *in vitro* modification by the C3 toxin. Anti-tubulin immunoblot serves as the loading control.

(C) Reconstitution of RhoA modification by bacteria-containing pellets of J2315-infected cell lysates. Pellets of lysates of DC2.4 cells infected with J2315 or Δ*hcp* were used as the source of activity to modify RhoA from non-infected DC2.4 cells. RhoA was subjected to further *in vitro* modification by the C3 toxin. Anti-tubulin immunoblot serves as the loading control.

(D) RhoA modification by lysates of J2315 but not *E. coli* and *B. thailandensis* (*B.t.*). RhoA from non-infected DC2.4 cells was incubated with the indicated bacterial lysates and subjected to further *in vitro* modification by the C3 toxin. Anti-tubulin immunoblot serves as the loading control.

(E) Asn-41 deamidation of RhoA in J2315 but not *E. coli*. WT or the N41A mutant RhoA was recombinantly expressed and purified from *B. cenocepacia* (WT or Δ*tecA*) or *E. coli*. The purified RhoA was subjected to further *in vitro* modification by the C3 toxin (upper) or mass spectrometry analyses. The lower panel shows the extracted ion chromatograms

of the Asn-41-containing peptide of RhoA from *B. cenocepacia* (*B.c.*) and *E. coli*. Spectrum 1/2 and 3/4 are from two separate experiments.

Figure 3. TecA Induces Rho Deamidation in Various Cellular Systems and Causes Actin Cytoskeleton Disruption.

(A and B) Modification of endogenous RhoA by TecA during *B. cenocepacia* infection. DC2.4 cells were infected with J2315 or the indicated mutant strains. Cell lysates were subjected to *in vitro* modification by the C3 toxin followed by immunoblotting analyses. An empty vector (Vec) or a plasmid expressing TecA was introduced into Δ*tecA* in (B).

(C) Ectopic expression of TecA in *B. thailandensis* induces endogenous RhoA modification during infection. DC2.4 cells were infected with *B. thailandensis* harboring an empty vector (Vec) or a TecA-expressing plasmid, or *B. cenocepacia* J2315 as a control. Assay of RhoA modification was performed similarly as that in (A). C41A is a catalytic cysteine mutant of TecA.

(D and E) Asn-41 deamidation of RhoA by TecA in transfected 293T cells. 293T cells were transfected with Myc-tagged TecA (WT or the C41A mutant). Endogenous RhoA modification in (D) was detected as in (A). In (E), cells were co-transfected with FLAG-RhoA and purified FLAG-RhoA was subjected to mass spectrometry analyses; shown are extracted ion chromatograms of the Asn-41-containing peptide.

(F) Asn-41 deamidation of RhoA by TecA co-expressed in *E. coli*. *E. coli* BL21 strain was transformed with two plasmids expressing His-RhoA and TecA (WT or the C41A mutant). Purified His-RhoA was subjected to mass spectrometry analyses and shown are extracted ion chromatograms of the Asn-41-containing peptide.

(G) Asn-39 deamidation of Rac1 by TecA in 293T cells. 293T cells were co-transfected with FLAG-Rac1 and Myc-TecA (WT or the C41A mutant). FLAG-Rac1 deamidation was assayed by mass spectrometry and extracted ion chromatograms of the Asn-39-containing peptide are shown.

(H) Deamidated Rac1 mimics TecA to alter the actin cytoskeleton structure. 293T cells were transfected with RhoA N41D or Rac1 N39D mutant together with EGFP as the transfection marker. Shown are the confocal fluorescence images of representative transfected cells. The arrows indicate "beads on a string"-like structures.

Figure 4. The TecA Family of Bacterial Proteins with Putative Cysteine Protease-like Fold and Catalytic Triad.

(A) ClustalW analysis of TecA orthologs ordered based on their sequence identity to TecA of *B. cenocepacia* K56-2 (which is 100% identical to TecA of J2315). TecA orthologs are present in *B. cenocepacia* (*B. ceno*), *B. contaminans* (*B. cont*), *B. pyrrocinia* (*B. pyrr*), *B. lata*, *B. cepacia* ATCC25416 (*B. cep*), *B. ubonensis* (*B. ubo*), *Alcaligenes faecalis*, *Chryseobacterium indologenes*, *Flavobacterium branchiophilum,* and *Ochrobactrum anthropi*. Conserved residues are depicted in red. Asterisks indicate the putative Cys-His-Asp catalytic triad residues.

(B) I*n silico* predicted structural model of *B. cenocepacia* K56-2 TecA, showing the location of the critical Cys-41 and His-105 residues of the putative catalytic triad. The Asp-148 is in a predicted unstructured region and therefore not indicated in the model.

Figure 5. TecA and Its Homologs Can Deamidate Rho GTPases *In Vitro*.

(A) Putative Cys-His-Asp catalytic triad residues are important for TecA modification of RhoA. 293T cells were transfected with Myc-TecA (WT or indicated mutants). Cell lysates were subjected to *in vitro* modification by the C3 toxin followed by immunoblotting. ΔC20 lacks the C-terminal 20 residues of TecA.

(B) RhoA modification by TecA homologs in 293T cells. 293T cells were transfected with mammalian expression plasmids encoding WP_034735953 (*C. indologenes*), WP_014085254 (*F. branchiophilum*) or WP_011982319 (*O. anthropi*). Cell lysates were subjected to *in vitro* modification by the C3 toxin followed by immunoblotting.

(C and D) Recombinant WP_034735953 from *C. indologenes* deamidates RhoA and Rac1 *in vitro*. Recombinant His-tagged WP_034735953 (WT or the catalytic cysteine mutant C40A) was incubated with purified RhoA or Rac1. Assay of RhoA modification by the C3 toxin in (C) was similar to that in (A). RhoA and Rac1 after incubation were analyzed by mass spectrometry. Shown in (D) are the extracted ion chromatograms of the peptide containing Asn-41 (for RhoA) or Asn-39 (for Rac1).

Figure 6. TecA Deamidation of RhoA Mediates *B. cenocepacia*-induced Pyrin Inflammasome Activation.

(A-D) TecA mediates *B. cenocepacia* infection-induced Pyrin inflammasome activation in its deamidase activity-dependent manner in mouse macrophages. Primary bone marrow-derived macrophage (BMDM) cells derived from WT (C57BL/6) or *Mefv*$^{-/-}$ mice were infected with wild-type *B. cenocepacia* J2315 or its Δ*tecA* mutant or stimulated with LPS plus nigericin (Nig) as a control. Cell supernatants were examined by immunoblotting with anti-caspase-1 in (A and C) (immunoblotting of tubulin in the cell

817 lysates serves as a loading control). Pro-Casp1, caspase-1 precursor; p10, the mature
818 caspase-1. ELISA of IL-1β release and pyroptotic cell death measured by LDH release
819 (n=3; mean ± SD) are shown in (B and D). In (C and D), Δ*tecA* was complemented with a
820 plasmid expressing WT TecA or the indicated catalytic mutants.
821 (E) TecA mediates *B. cenocepacia* infection-induced Pyrin inflammasome activation in
822 DC2.4 cells. DC2.4 cells stably expressing Pyrin were infected with *B. cenocepacia*
823 J2315 or the indicated mutant and complementation strains similarly as in (A and C). Cell
824 supernatants were examined by anti-caspase-1 immunoblotting; immunoblotting of
825 tubulin in the cell lysates serves as a loading control. Pro-Casp1, caspase-1 precursor;
826 p10, the mature caspase-1.
827 (F) A deamidation-resistant mutant RhoA inhibits *B. cenocepacia*-induced Pyrin
828 inflammasome activation. DC 2.4 cells stably expressing FLAG-tagged wild-type RhoA
829 or the denoted N/L mutant of RhoA, Rac1 or Cdc42 were infected with *B. cenocepacia*
830 J2315. The supernatant were subjected to anti-caspase-1 immunoblotting.
831 Immunoblotting of tubulin in cell lysates serves as a loading control. Anti-FLAG
832 immunoblot in the lower panel shows the expression of exogenous Rho GTPases. Pro-
833 Casp1, caspase-1 precursor; p20, the mature caspase-1.
834
835 **Figure 7. The Rho Deamidase Activity of TecA Triggers Inflammation and Its**
836 **Recognition by Pyrin Protects Mice from Lethal *B. cenocepacia* Infection.**
837 (A and B) WT C57BL/6 mice were infected with *B. cenocepacia* J2315 wild-type strain,
838 or Δ*tecA*, or Δ*tecA* containing a plasmid expressing TecA (WT or the C41A mutant).
839 Representative haematoxylin & eosin staining of the lung sections is shown in (A).

840 Quantification scores of the lung injury ((n=2; mean ± SD) are shown in (B). Data shown
841 are representative of two independent repetitions.
842 (C) Survival of mice (WT and *Mefv*$^{-/-}$) following peritoneal infection of *B. cenocepacia*
843 J2315 (wild-type or the Δ*tecA* strain). Survival curve analysis was performed with the
844 log-rank (Mantel–Cox) test in GraphPad Prism 5 (*P $\leqslant$ 0.05). Data shown are
845 representative of three independent experiments.
846 (D) Bacterial loads in the spleen and liver of mice intraperitoneally infected with *B.*
847 *cenocepacia* J2315 (wild-type or the Δ*tecA* strain). Colony-forming units (CFUs) per
848 gram of tissues 4 days after infection are shown as mean values (n=7). *P $\leqslant$ 0.05; ns,
849 non-significant (two-tailed unpaired Student's *t*-test).

Figure 1. Identification of *tecA* Encoding A Novel Non-VgrG T6SS Effector Functioning in Eukaryotic Host Cells

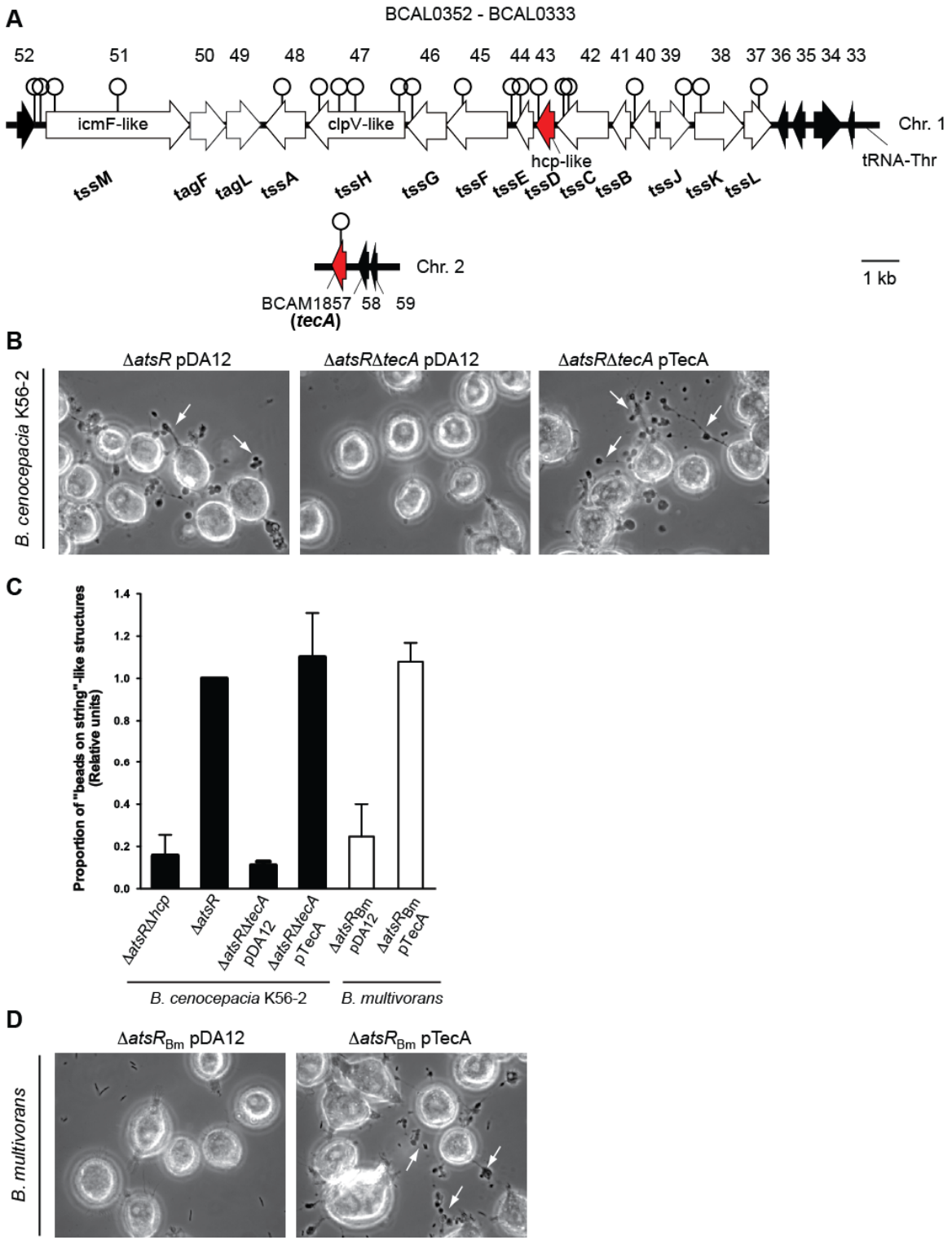

Figure 2. A T6SS-dependent Activity in *B. cenocepacia* That Leads to Rho Deamidation

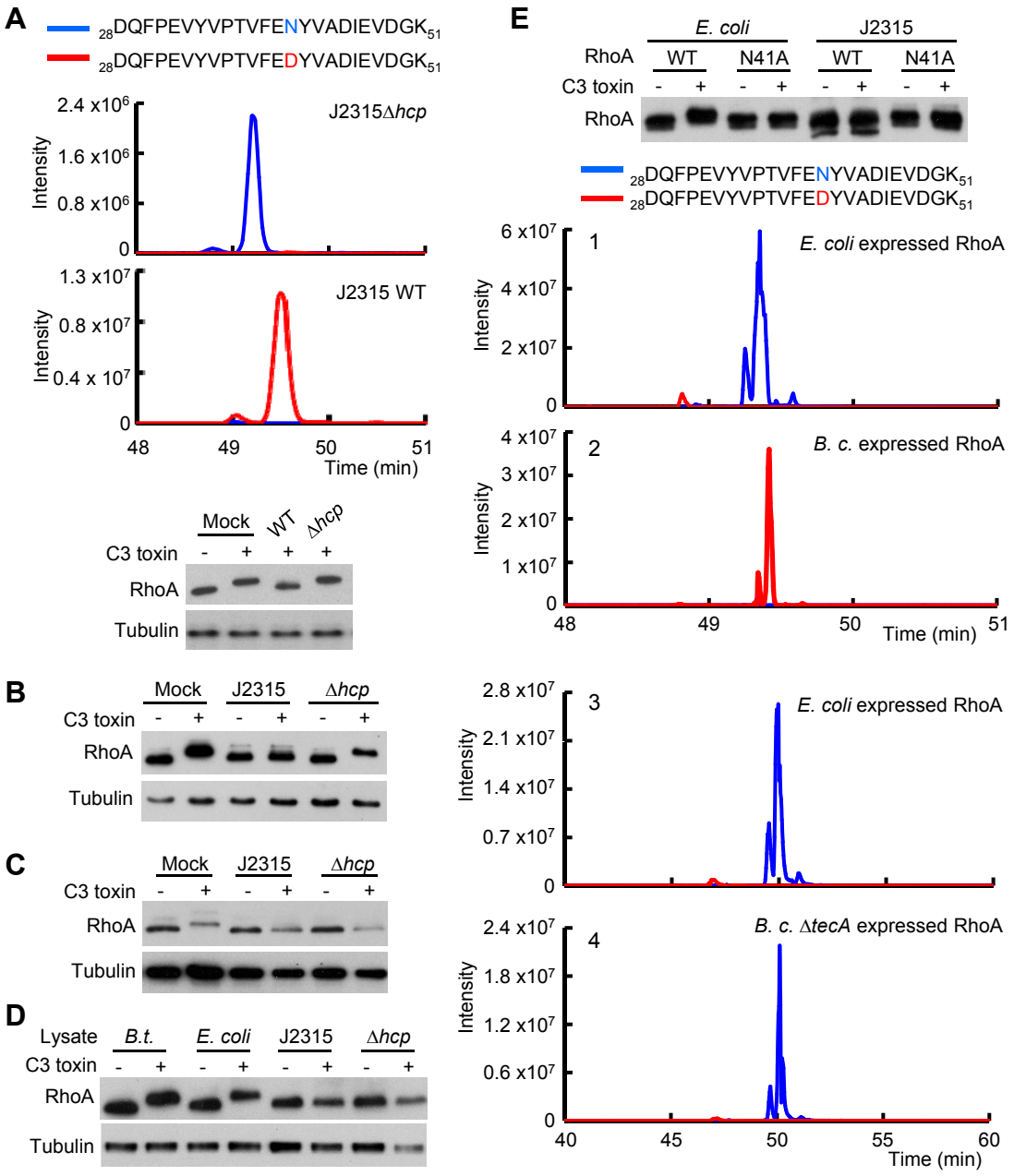

Figure 3. TecA Induces Rho Deamidation in Various Cellular Systems and Causes Actin Cytoskeleton Disruption

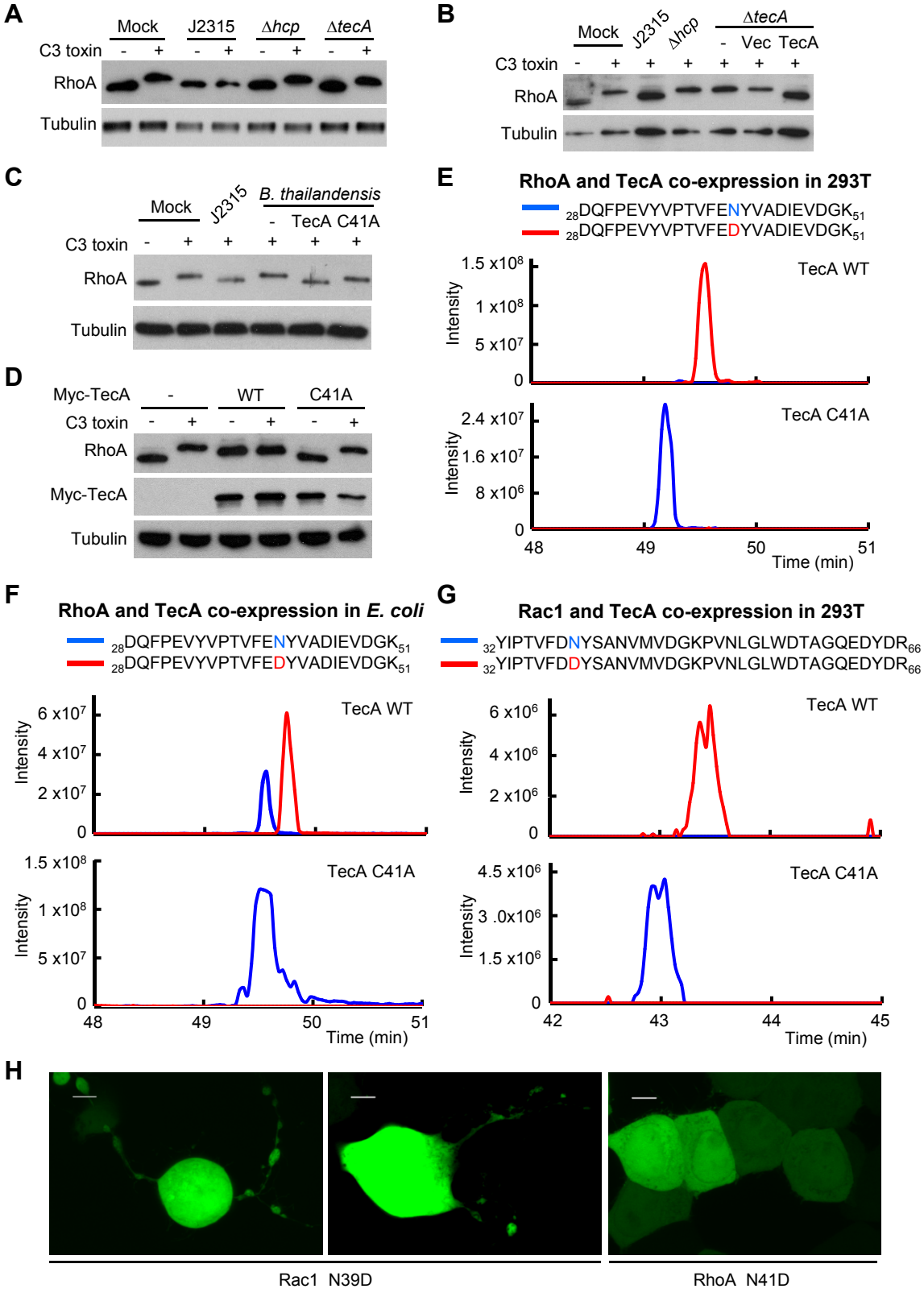

Figure 4. The TecA Family of Bacterial Proteins with Putative Cysteine Protease-like Fold and Catalytic Triad

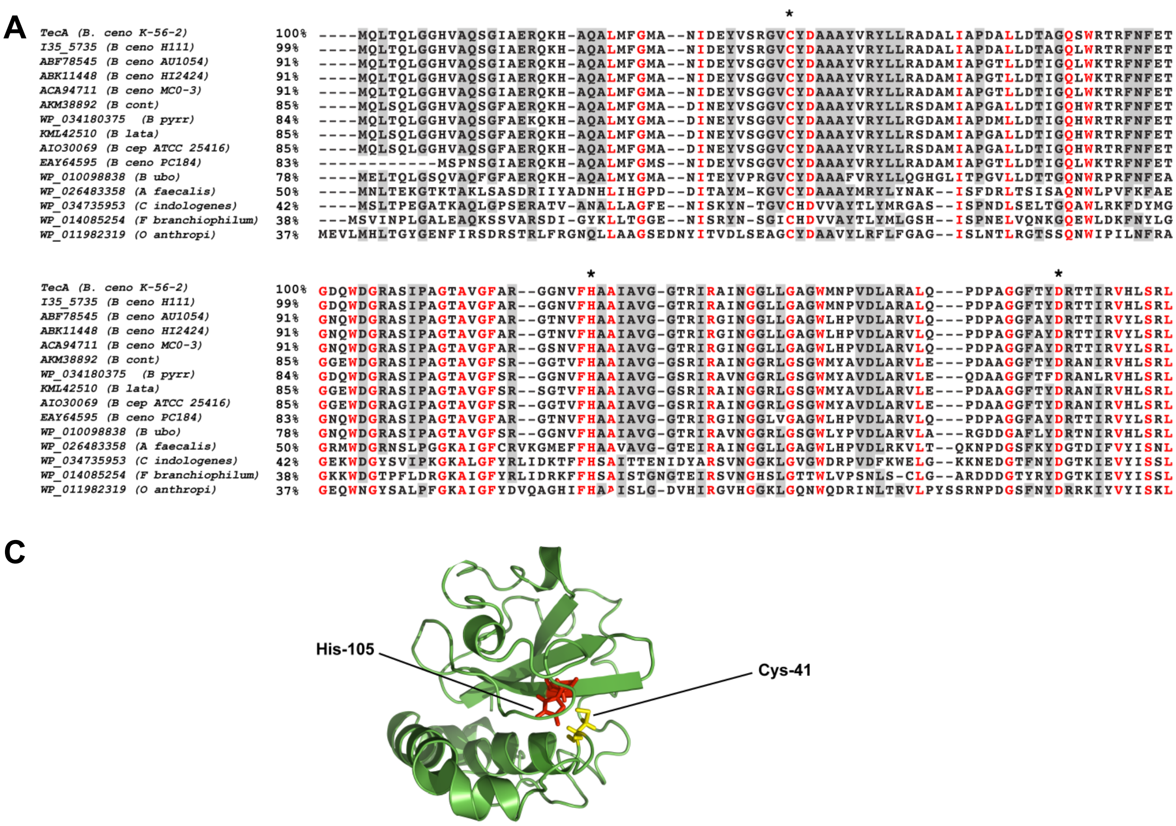

Figure 5. TecA and Its Homologs Can Deamidate Rho GTPases *In Vitro*

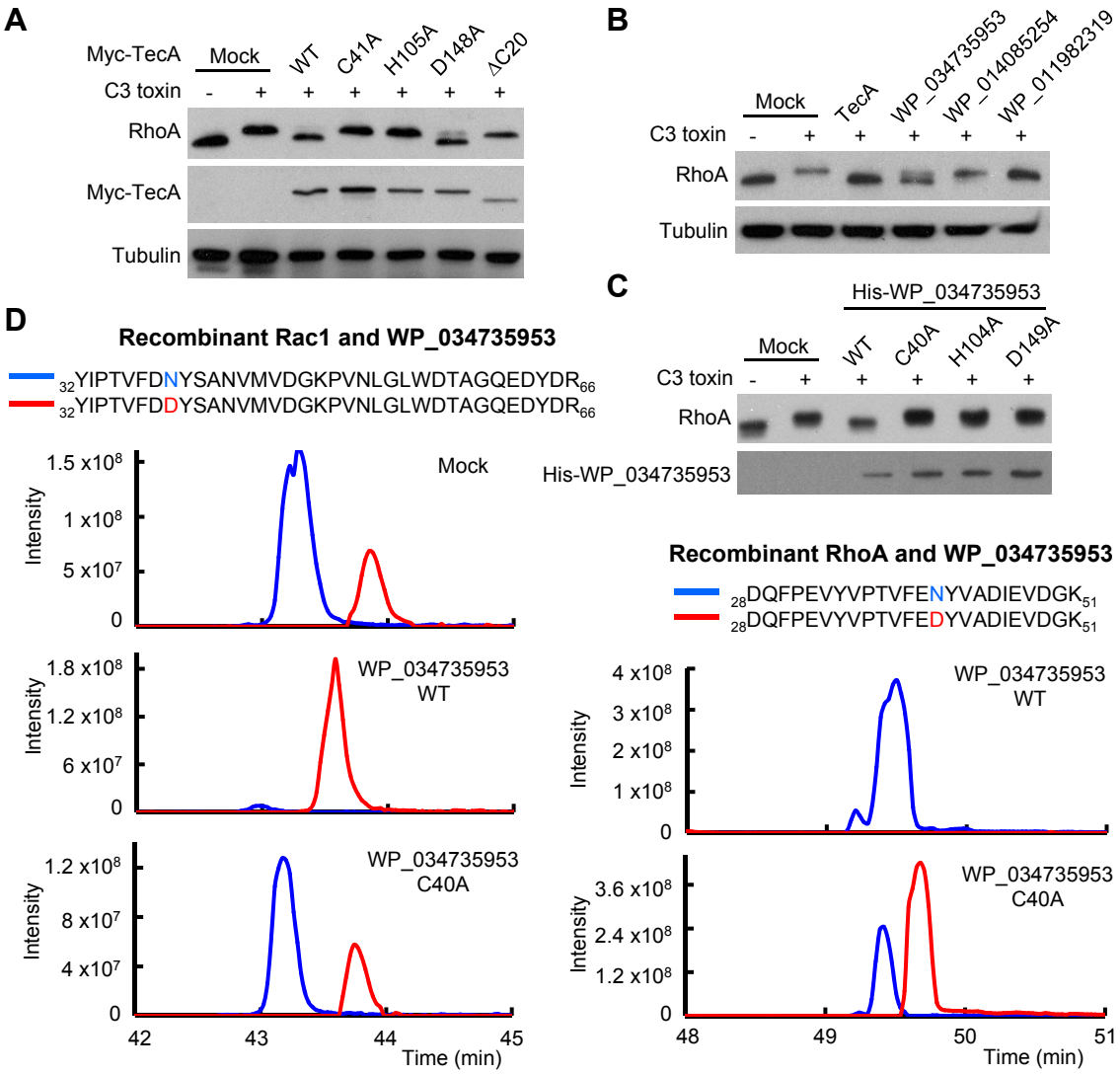

Figure 6. TecA Deamidation of RhoA Mediates *B. cenocepacia*-induced Pyrin Inflammasome Activation

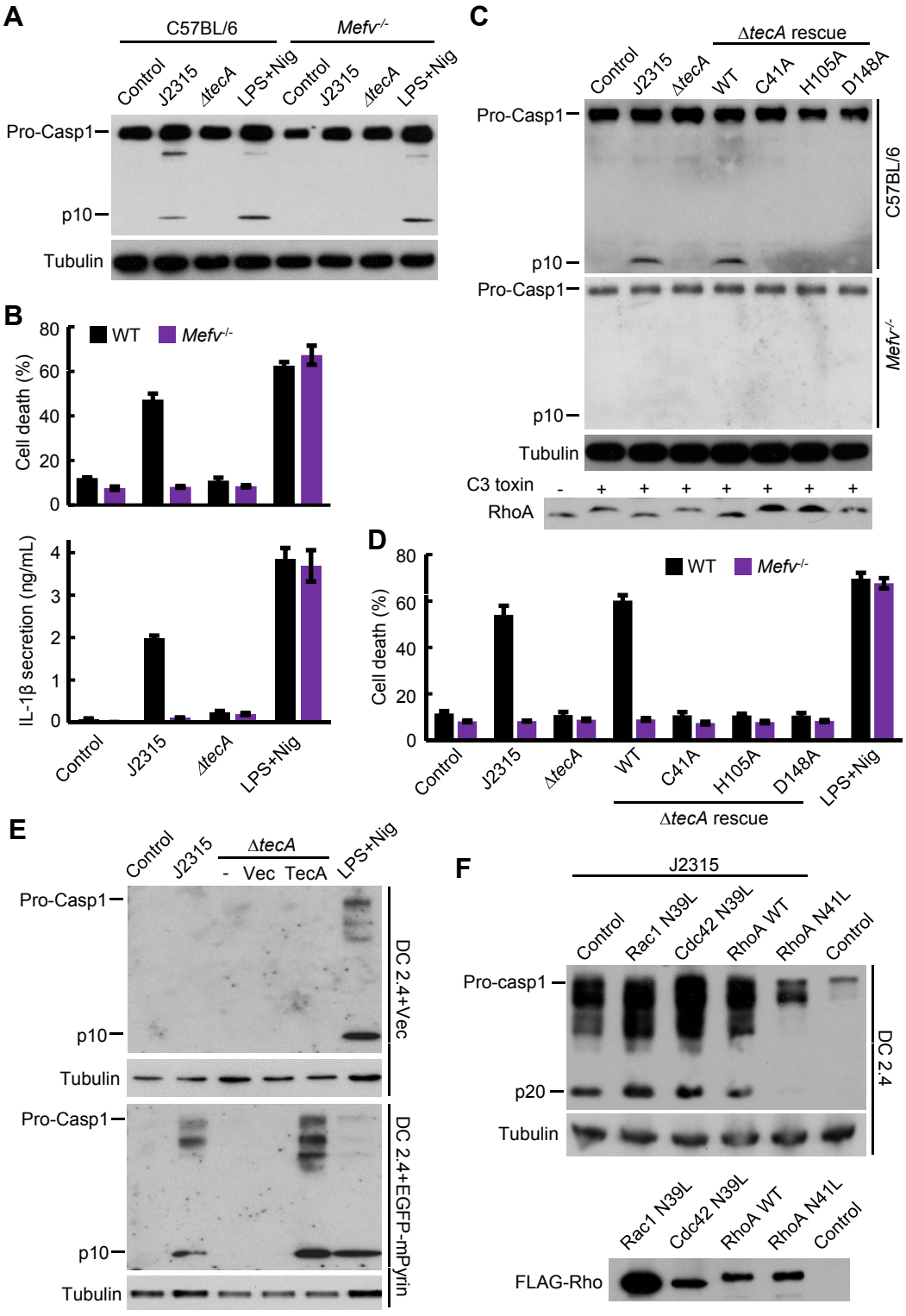

Figure 7. The Rho Deamidase Activity of TecA Triggers Inflammation and Its Recognition by Pyrin Protects Mice from Lethal *B. cenocepacia* Infection

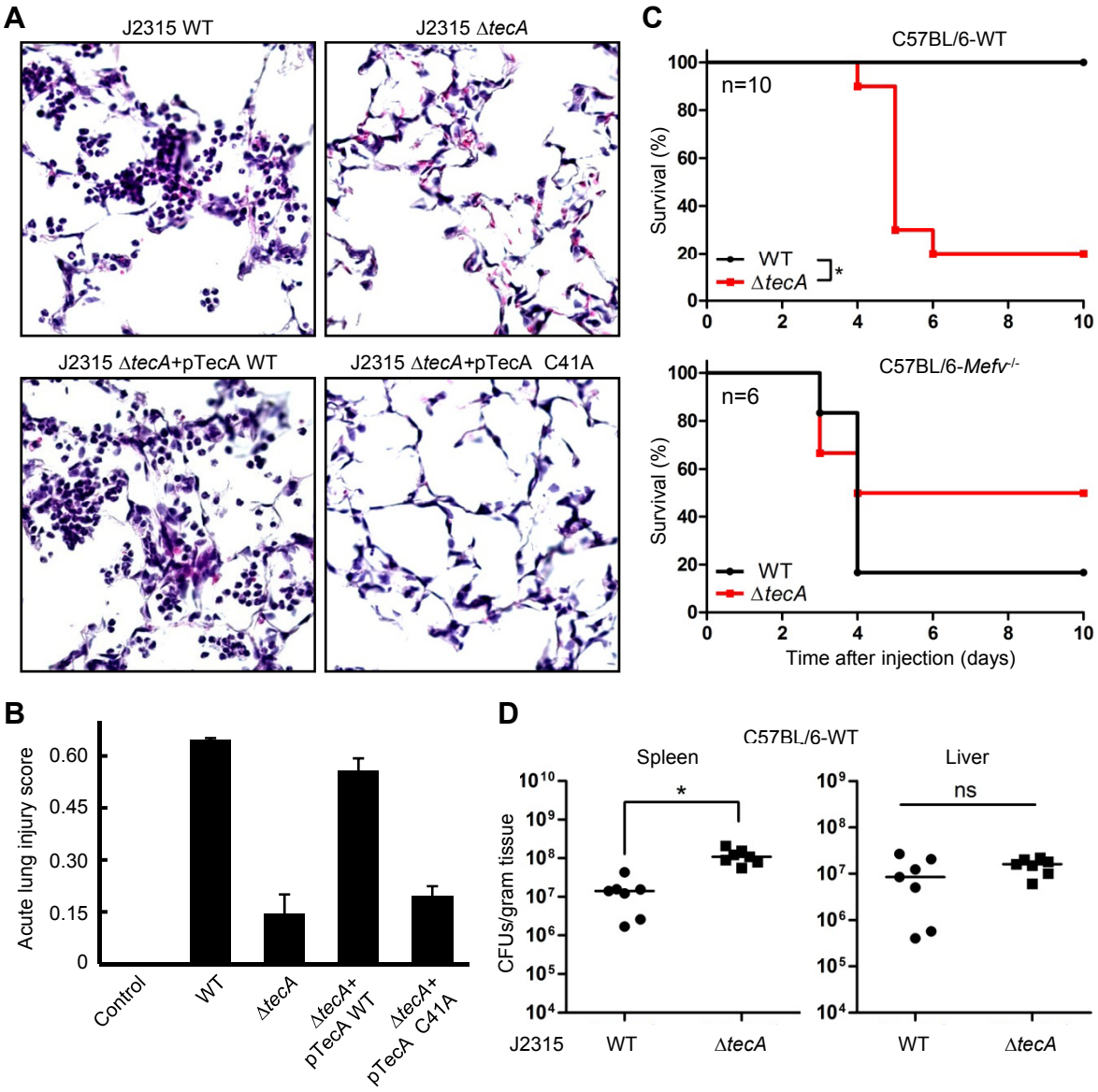

Figure S1. Characterization of *B. cenocepacia* K56-2 Δ*tecA* Mutant and T6SS-dependent TecA Secretion